Interactions of Nucleotide Cofactors with the *Escherichia coli* Replication Factor DnaC Protein†

Roberto Galletto, Surendran Rajendran, and Wlodzimierz Bujalowski*

Department of Human Biological Chemistry & Genetics, The University of Texas Medical Branch at Galveston, Galveston, Texas 77555-1053

Received May 31, 2000; Revised Manuscript Received August 16, 2000

ABSTRACT: Quantitative analyses of the interactions of nucleotide cofactors with the *Escherichia coli* replicative factor DnaC protein have been performed using thermodynamically rigorous fluorescence titration techniques. This approach allowed us to obtain stoichiometries of the formed complexes and interaction parameters, without any assumptions about the relationship between the observed signal and the degree of binding. The stoichiometry of the DnaC−nucleotide complex has been determined in direct binding experiments with fluorescent nucleotide analogues, MANT-ATP and MANT-ADP. The stoichiometry of the DnaC complexes with unmodified ATP and ADP has been determined using the macromolecular competition titration method (MCT). The obtained results established that at saturation the DnaC protein binds a single nucleotide molecule per protein monomer. Analyses of the binding of fluorescent analogues and unmodified nucleotides to the DnaC protein show that ATP and ADP have the same affinities for the nucleotide-binding site, albeit the corresponding complexes have different structures, specifically affected by the presence of magnesium cations in solution. Although the presence of the γ-phosphate does not affect the affinity, the structure of the triphosphate group is critical. While the affinity of ATP-γ-S is the same as the affinity of ATP, the affinities of AMP−PNP and AMP−PCP are ∼2 and ∼4 orders lower than that of ATP, respectively. Moreover, the ribose plays a significant role in forming a stable complex. The binding constants of dATP and dADP are ∼2 orders of magnitude lower than those for ribose nucleotides. The nucleotide-binding site of the DnaC protein is highly base specific. The intrinsic affinity of adenosine triphosphates and diphosphates is at least 3−4 orders of magnitude higher than for any of the other examined nucleotides. The obtained data indicate that the recognition mechanism of the nucleotide by the structural elements of the binding site is complex with the base providing the specificity and the ribose, as well as the second phosphate group contributing to the affinity. The significance of the results for the functioning of the DnaC protein is discussed.

The DnaC protein is an essential replication protein in *Escherichia coli* (*1*−*5*). Both fast- and slow-stop mutations of the protein have been identified indicating that the protein is involved in initiation and elongation stages of the chromosomal DNA replication, as well as in the replication of phage and plasmid DNAs (*1*−*7*). The DnaC protein participates in the formation of the replication fork as well as in the assembly of the primosome, a multiple-protein−DNA complex, which can translocate along the DNA while synthesizing short oligoribonucleotide primers that are used to initiate synthesis of the complementary strand (*1*, *2*, *8*). In these capacities, the DnaC protein specifically interacts under ATP[1] control with the *E. coli* primary replicative helicase, the DnaB protein, allowing the helicase to recognize specific protein−DNA complexes, most probably through interactions with other replication proteins (*1*, *9*−*14*). The DnaC protein is not necessary for the DnaB helicase to bind the ssDNA. The helicase can form a complex with the nucleic acid with significant affinity without DnaC (*16*−*21*). Thus, the formation of the DnaC−DnaB complex allows the helicase to recognize the DNA sequence of the replication origin, oriC, complexed with the replication initiation factor, the DnaA protein (*1*, *3*, *9*, *11*, *12*). The DnaC protein is absolutely required for this reaction (*1*, *3*, *9*). In the formation of the primosome, the DnaC−DnaB complex allows the helicase to recognize a specific multi-protein−DNA complex, which includes PriA, PriB, PriC, and DnaT proteins at the primosome assembly site (PAS) (*12*, *21*). Due to its highly specific role in "delivering" the replication helicase to specific replication complexes and the ATP requirement for these reactions, the DnaC protein has been termed "molecular matchmaker" (*22*).

The DnaC protein was originally isolated based on its requirement for in vitro ϕX174 phage replication (*4*, *5*). The

† This work was supported by NIH Grants GM-46679 and GM-58675 (to W.B.).

* To whom correspondence should be addressed. Phone: (409) 772-5643. Fax: (409) 772-1790. E-mail: wbujalow@utmb.edu.

[1] Abbreviations: ATP, adenosine 5′-triphosphate; ADP, adenosine 5′-diphosphate; dATP, 2′-deoxyadenosine 5′-triphosphate; dADP, 2′-deoxyadenosine 5′-diphosphate; AMP−PNP, β,γ-imodoadenosine 5′-triphosphate; AMP−PCP, β,γ-methylene-adenosine 5′-triphosphate; TNP-ATP, 2′(3′)-*O*-(2,4,6-trinitrophenyl)adenosine 5′-triphosphate; MANT-ATP, 3′-*O*-(*N*-methylantraniloyl)-5′-triphosphate; MANT-ADP, 3′-*O*-(*N*-methylantraniloyl)-5′-diphosphate; ATPγS, adenosine 5′-*O*-(3-thiotriphosphate); Tris, tris(hydroxymethyl)aminomethane; DTT, dithiothreitol; DEAE-cellulose, diethylaminoethyl-cellulose.

10.1021/bi0012484 CCC: $19.00
Published on Web 09/21/2000

gene encoding the DnaC protein has been cloned (*13*, *14*, *23*). Its sequence, and that of the encoded protein, have been determined (*23*). The native protein is a monomer with a molecular mass of 27 894 kDa (*23*).

Current views on the role of the DnaC protein in DNA replication strictly relate it to the highly specific interactions of the protein with the *E. coli* primary replicative helicase, the DnaB protein, which are under ATP control (*1*−*5*, *9*, *10*, *24*−*26*). In contrast, ADP does not support these interactions. Hydrolysis of ATP is not necessary for the complex formation, although this has not been rigorously proven. The DnaC protein does not have intrinsic ATPase activity. These results suggest that ATP acts as a positive effector inducing conformational changes in the DnaC protein and increasing its affinity for the helicase, while ADP acts as a negative effector.

Elucidation of nucleotide interactions with the DnaC protein and their regulatory role is of paramount importance for our understanding of the activities of this essential replication factor. Although the importance of nucleotide cofactors in controlling the DnaC protein activities has been recognized, the mechanism and nature of this control remain obscure, particularly at the molecular level. It has been suggested, on the basis of equilibrium gel filtration, that the DnaC protein binds close to one ATP molecule with an affinity of $\sim 10^5-10^6$ M^{-1} (*9*). The stoichiometry and affinity of the protein for the negative effector, ADP, has never been addressed. There is also a significant controversy concerning the fundamental problem of the base specificity of the DnaC protein. While strong specificity of the DnaC nucleotide-binding site for ATP has been found by some authors (*9*), lack of any base specificity has been proposed by others (*27*). The affinities of different nucleotides for the DnaC protein have never been addressed.

In this communication, we quantitatively examine the interactions of nucleotide cofactors with the DnaC protein, using fluorescent nucleotide analogues, MANT-ATP, MANT-ADP, MANT-GDP, MANT-UDP, MANT-CDP, TNP-ATP, and unmodified nucleotides (*28*−*32*). Quantitative analyses of the interactions of the nucleotides with the DnaC protein have been performed using thermodynamically rigorous fluorescence titration techniques. The obtained results establish that at saturation the DnaC protein binds a single nucleotide molecule per protein monomer. Moreover, ATP and ADP have, within experimental accuracy, the same affinities for the protein. The nucleotide-binding site of the DnaC protein is highly specific for adenosine nucleotides. The intrinsic affinity of ATP and ADP is ∼3−4 orders of magnitude higher than for any other nucleotide. The data indicate that the nucleotide-binding site is strongly hydrophobic in nature. The recognition mechanism of the nucleotide by the structural elements of the binding site is a complex process, which includes allosteric interactions with magnesium binding sites.

MATERIALS AND METHODS

Reagents and Buffers. All chemicals were of reagent grade. All solutions were made with distilled and deionized 18 MΩ (Milli-Q) water. The standard buffer, T4, is 50 mM Tris adjusted to pH 8.1 at appropriate temperatures with HCl, 5 mM $MgCl_2$, 10% glycerol, and 1 mM DTT. The temperature and concentrations of NaCl in the buffer are indicated in the text.

Nucleotides. MANT-ATP, MANT-ADP, MANT-GDP, MANT-CDP, and MANT-UDP were synthesized as described (*30*−*33*). Fluorescent nucleotide analogues used in the binding studies were >95% pure as judged by TLC on silica. ATP and ADP were from CalBiochem. TTP, GTP, CTP, UTP, AMP−PCP, AMP−PNP, and ATP-γ-S were from Sigma.

DnaC Protein. The plasmid pET3c harboring the *E. coli* DnaC protein gene was a generous gift from Dr. K. Marians (Sloan Kettering). However, we determined that the gene contained the D6A mutation, where the sixth amino acid was aspartic acid instead of alanine, as indicated by the published nucleotide sequence (*23*). We changed the mutation back to alanine. Moreover, to obtain better overproduction, we placed the gene in the plasmid pET30a (Novagen).

Protein Purification. The DnaC protein was purified from overproducing cells by the following procedure. The cells were first disrupted by temperature shock, followed by the addition of 0.03% (w/v) sodium deoxycholate. Brij 58 was added to the isolation buffers at the 0.002% (w/v) concentration to preserve protein stability, although we found no effect on protein stability and activity when Brij 58 was either included or omitted in the thermodynamic studies described in this work. The cell extract was dialyzed overnight against buffer A (50 mM Tris/HCl, pH 8.1, 10% glycerol, 0.002% Brij 58, 1 mM DTT) and subsequently loaded on a phosphocellulose column (P11, Whatman). The column was first eluted with buffer A containing 50 mM NaCl, then with the same buffer containing 150 mM NaCl, and the fraction with the DnaC protein was eluted with buffer A containing 500 mM NaCl (Fraction 1). Fraction 1 was precipitated with ammonium sulfate, redissolved in buffer A, and dialyzed overnight against buffer B (50 mM Tris/HCl pH 8.1, 10% glycerol, 0.002% Brij 58, 1 mM DTT, 20 mM NaCl). The sample was subsequently loaded on the DEAE-cellulose column, eluted in the same buffer, precipitated with ammonium sulfate, and redissolved in storage buffer C (50 mM Tris/HCl pH 8.1, 50% glycerol, 0.01% Brij 58, 150 mM NaCl). The DnaC protein was >97% pure as judged by SDS−acrylamide gel electrophoresis with Coomasie Brilliant Blue staining. The concentration of the protein was spectrophotometrically determined with the extinction coefficient $\epsilon_{280} = 23.2 \times 10^4$ M^{-1} cm^{-1} (monomer) determined using an approach based on the Edelhoch method (*34*, *35*).

Fluorescence Measurements. All fluorescence titrations were performed using SLM 48000S or SLM 8100 spectrofluorometers. To avoid possible artifacts, due to the fluorescence anisotropy of the sample, polarizers were placed in excitation and emission channels and set at 90 and 54.7° (magic angle), respectively. The binding was followed by monitoring the fluorescence increase of the nucleotide analogues with $\lambda_{ex} = 356$ nm and $\lambda_{em} = 450$ nm. All titration points were corrected for dilution and inner filter effects using the following formula (*30*, *36*)

$$F_{cor} = (F_i - B_i)\left(\frac{V_i}{V_o}\right)10^{0.5b(A_{\lambda_{ex}}+A_{\lambda_{em}})} \qquad (1)$$

where F_{cor} is the corrected value of the fluorescence intensity at a given point of titration i, F_i is the experimentally

measured fluorescence intensity, B_i is the background, V_i is the volume of the sample at a given titration point, V_o is the initial volume of the sample, b is the total length of the optical path in the cuvette expressed in centimeters, and $A_{i_{\lambda ex}}$ and $A_{i_{\lambda em}}$ are the absorbances of the sample at excitation and emission wavelengths, respectively. Analyses of the binding isotherms and computer simulations were performed using KaleidaGraph software (Synergy Software, PA).

Determination of Thermodynamically Rigorous Binding Isotherms. In the experiments described in this work we measured the binding of fluorescent analogue nucleotides to the DnaC protein by following the fluorescence increase of MANT-analogues titrated with the protein. This type of titration is referred to as the reverse titration method (*37*). Our studies showed that a single molecule of the nucleotide binds per DnaC protein (see below). However, this stoichiometry has been established by determining the relationship between the observed nucleotide analogue fluorescence, ΔF, and the average number of bound DnaC protein molecules per nucleotide, $\sum\Theta_i$, without any assumption as to the relationship between the observed spectroscopic signal and $\sum\Theta_i$. To achieve this, we applied an approach previously described by us (*16*−*20*, *37*, *38*). Briefly, the experimentally observed ΔF has a contribution from each of the different possible "*i*" complexes of the nucleotide analogue with the DnaC protein. The observed fluorescence increase, ΔF, is related to $\sum\Theta_i$ by (*16*−*20*)

$$\Delta F = \sum \Theta_i \Delta F_{i_{max}} \tag{2}$$

where $\Delta F_{i_{max}}$ is the molecular parameter characterizing the maximum fluorescence increase of the analogue with the DnaC protein bound in complex "*i*". The same value of ΔF, obtained at two different total nucleotide concentrations, N_{T_1} and N_{T_2}, indicates the same physical state of the analogue, i.e., the degree of binding, $\sum\Theta_i$, and the free protein concentration, P_F, must be the same. The value of $\sum\Theta_i$ and P_F is then related to the total protein concentrations, P_{T_1} and P_{T_2}, and the total nucleotide concentrations, N_{T_1} and N_{T_2}, at the same value of ΔF, by

$$\sum \Theta_i = \frac{P_{T_2} - P_{T_1}}{N_{T_2} - N_{T_1}} \tag{3a}$$

$$P_F = P_T - (\sum \Theta_i) N_{T_x} \tag{3b}$$

where $x = 1$ or 2 (*15*−*20*, *37*, *38*).

It should be noted that it is necessary to apply the procedure to the binding system in order to establish the relationship between ΔF and $\sum\Theta_i$ and to verify that it is true over the range of studied solution conditions. The obtained relationship can then be used to determine true binding parameters from a single titration curve by simply converting it to a quantitative binding isotherm, i.e., a plot of the average degree of binding as a function of the protein concentration.

Quantitative Analysis of DnaC Protein-Unmodified Nucleotide Interactions Using the MCT Method. Thermodynamics of the DnaC−unmodified nucleotide (e.g., ATP and ADP) complexes has been addressed using the MCT method (*17*, *33*). Briefly, if the fluorescent reference ligand (e.g., MANT-ADP) at total concentration, N_{T_R}, is titrated with the protein in the presence of a competing nonfluorescent nucleotide at total concentration, N_{1_S}, the total concentration of the protein, P_{T_1}, at which a given fluorescence change, ΔF_i, is observed, is described by

$$P_{T_1} = (\sum \Theta_i)_S N_{1_S} + (\sum \Theta_i)_R N_{T_R} + P_F \tag{4a}$$

where $(\sum\Theta_i)_R$, $(\sum\Theta_i)_S$, and P_F are the number of protein molecules bound to a reference nucleotide, the number of the protein molecules bound to the nonfluorescent, competing nucleotide and the free protein concentration. The total concentration of the protein, P_{T_2}, at which the same ΔF_i is observed at the same N_{T_R}, but with a different total concentration of the competing nucleotide, N_{2_S}, is described by

$$P_{T_2} = (\sum \Theta_i)_S N_{2_S} + (\sum \Theta_i)_R N_{T_R} + P_F \tag{4b}$$

Subtracting eq 4a from 4b and rearranging provides eq 5 that allows us to determine the average number of protein molecules associated with the unmodified nucleotide as

$$(\sum \Theta_i)_S = \frac{P_{T_2} - P_{T_1}}{N_{2_S} - N_{1_S}} \tag{5}$$

RESULTS

Stoichiometry of the Nucleotide−DnaC Protein Complex. Binding of unmodified nucleotide cofactors, ATP and ADP, to the DnaC protein is not accompanied by an adequate fluorescence change that enables a quantitative analysis of the interactions to be performed. However, we found that binding of the fluorescent analogues, MANT-ATP or MANT-ADP, to the protein is accompanied by a strong increase of the analogue fluorescence (see below). Also, there is a blue shift of the emission spectra (data not shown). For MANT-nucleotides saturated with the DnaC protein, the maximum of the emission spectrum is located at $\lambda = 441$ nm, as compared to $\lambda = 450$ nm for the free nucleotides. Such a large fluorescence emission increase and blue shift of the spectra in the complex with the DnaC protein indicate that, in the binding site, the MANT residue is located in a strongly hydrophobic environment (*31*, *33*).

Fluorescence titrations of MANT-ATP with the DnaC protein, at three different nucleotide concentrations, in buffer T4 (pH 8.1, 20 °C), containing 100 mM NaCl, are shown in Figure 1a. At higher nucleotide concentrations, a given relative fluorescence increase is reached at higher DnaC protein concentrations. This results from the fact that at higher analogue concentrations more protein is required to obtain the same degree of binding, $\sum\Theta_i$. The selected MANT-ATP concentrations provide separation of the binding isotherms up to the relative fluorescence increase of $\Delta F \approx 1.3$.

To obtain thermodynamically rigorous binding parameters, independently of any assumption about the relationship between the observed signal and the degree of binding, $\sum\Theta_i$, the fluorescence titration curves, shown in Figure 1a, have been analyzed, using the approach outlined in Materials and Methods (*15*−*20*, *33*). Figure 1b shows the dependence of the observed relative fluorescence increase of MANT-ATP

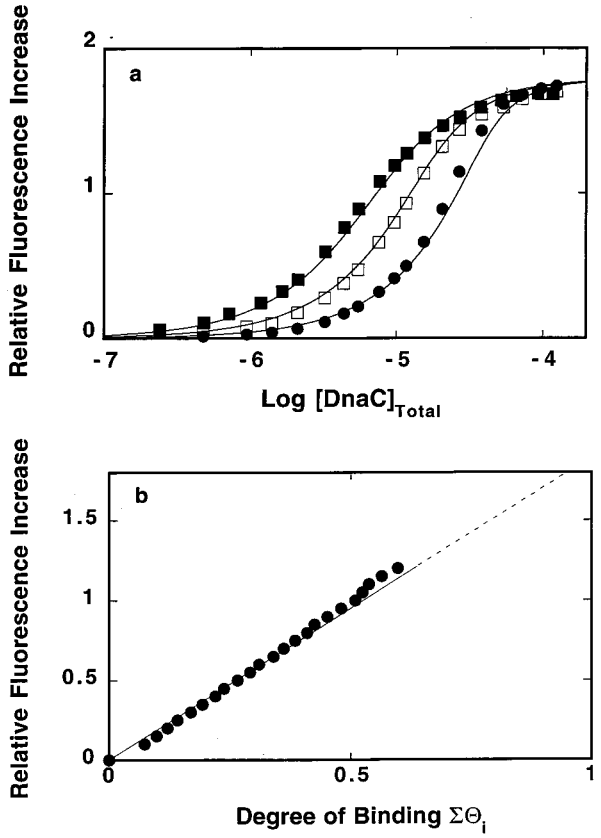

FIGURE 1: (a) Fluorescence titration of MANT-ATP with the DnaC protein, in buffer T4 (pH 8.1, 20 °C), containing 100 mM NaCl, at different MANT-ATP concentrations: (■) 5.7×10^{-6} M; (□) 1.5×10^{-5} M; (●) 4×10^{-5} M. The solid lines are computer fits of the titration curves, using a single set of binding parameters (eq 6) with the intrinsic binding constant $K = 3 \times 10^5$ M^{-1} and the relative fluorescence change $\Delta F_{max} = 1.8$. (b) Dependence of the relative fluorescence increase of MANT-ATP, and ΔF upon the average number of bound DnaC protein, $\sum\Theta_i$ (●). The values of $\sum\Theta_i$ have been determined using the thermodynamically rigorous approach described in Materials and Methods. The solid line follows the experimental points and has no theoretical basis. The dashed line is the extrapolation of ΔF to the maximum value of $\Delta F_{max} = 1.8$.

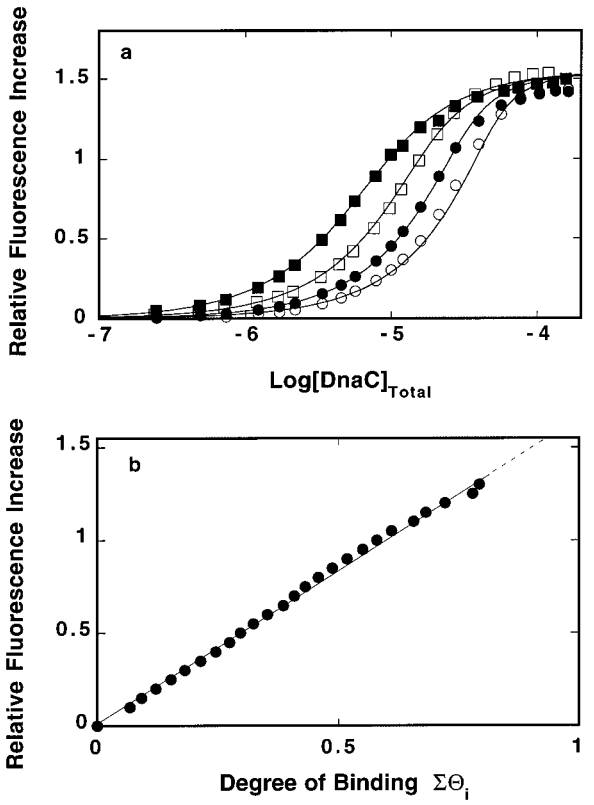

FIGURE 2: (a) Fluorescence titration of MANT-ADP with the DnaC protein, in buffer T4 (pH 8.1, 20 °C) containing 100 mM NaCl, at different MANT-ADP concentrations: (■) 5.6×10^{-6} M; (□) 1.5×10^{-5} M; (●) 3×10^{-5} M; (○) 5×10^{-5} M. The solid lines are computer fits of the titration curves, using a single set of binding parameters (eq 6), with the intrinsic binding constant $K = 3 \times 10^5$ M^{-1} and relative fluorescence change $\Delta F_{max} = 1.55$. (b) Dependence of the relative fluorescence increase of MANT-ADP and ΔF upon the average number of bound DnaC protein, $\sum\Theta_i$ (●). The values of $\sum\Theta_i$ have been determined using the thermodynamically rigorous approach described in Materials and Methods. The solid line follows the experimental points and has no theoretical basis. The dashed line is the extrapolation of ΔF to the maximum value of $\Delta F_{max} = 1.55$.

as a function of the average degree of binding of the DnaC protein. The obtained binding isotherms allow us to determine $\sum\Theta_i$ up to ~65% of the total fluorescence increase (Figure 1b). The plot is linear, indicating that the fluorescence change is constant over the entire binding process. Extrapolation to the maximum fluorescence change, $\Delta F_{max} = 1.8 \pm 0.1$, shows that at saturation only one molecule of MANT-ATP binds to the DnaC protein.

Fluorescence titrations of MANT-ADP with the DnaC protein, at four different nucleotide concentrations, in buffer T4 (pH 8.1, 20 °C), containing 100 mM NaCl, are shown in Figure 2a. The maximum increase of the MANT-ADP fluorescence, $\Delta F_{max} = 1.55 \pm 0.1$, upon saturation with the DnaC protein, is lower than $\Delta F_{max} = 1.8 \pm 0.1$ obtained for MANT-ATP (see Figure 1, panels a and b). Such a difference in the emission intensity indicates different conformational states of ATP versus ADP, when bound to the DnaC protein (*31*, *33*). The dependence of the observed relative fluorescence increase of MANT-ADP, as a function of the average degree of binding, $\sum\Theta_i$, of the DnaC protein, is shown in Figure 2b. Similar to MANT-ATP (Figure 1b), the plot is linear, indicating that over the entire binding process, the fluorescence change is constant. Extrapolation to the maximum fluorescence change, $\Delta F_{max} = 1.55$, shows that at saturation only one molecule of MANT-ADP binds to the DnaC protein.

Intrinsic Affinities of MANT-ATP and MANT-ADP Complexes with the DnaC Protein. Knowing the stoichiometry of the protein−nucleotide complex, we can address the intrinsic affinities of the nucleotide. Fluorescence titration curves presented in Figures 1 and 2 can be analyzed using single-site binding isotherms as described by

$$\Delta F = \Delta F_{max}\left(\frac{K_N P_F}{1 + K_N P_F}\right) \qquad (6)$$

where K_N is the binding constant for MANT-ATP and MANT-ADP, and P_F is the free DnaC concentration. The solid lines in Figures 1a and 2a are the computer fits using eq 6. Within experimental accuracy, the obtained values of the binding constants are the same with $K_{MANT-ATP} = K_{MANT-ADP} = (3 \pm 0.4) \times 10^5$ M^{-1}. These data show, for the first time, that the DnaC protein has the same affinities for both ATP and ADP analogues. Rigorous competition

titration studies using unmodified ATP and ADP fully confirm these results (see below).

Affinities of ATP and ADP for the DnaC Protein. Analyses Using the Macromolecular Competition Titration Method (MCT). As we mentioned above, binding of ATP and ADP to the DnaC protein is not accompanied by a protein fluorescence change adequate enough to quantitatively determine the energetics of the interactions. However, stoichiometries and intrinsic affinities of the unmodified ATP and ADP can be rigorously determined using the MCT method (*17*, *33*). This model-independent method is based on the same thermodynamic arguments as applied to titrations of fluorescent analogues with the protein. In the presence of the competing, unmodified nucleotide, the protein binds to two different cofactors present in solution, but the observed signal originates only from the fluorescent "reference" cofactor. As the titration progresses, and the free protein concentration increases in the sample, the saturation of both nucleotides increases (*33*).

In studies reported in this work, we use MANT-ADP as a reference fluorescent ligand (*33*). Fluorescence titrations of MANT-ADP with the DnaC protein in the presence of two different concentrations of ATP, in buffer T4 (pH 8.1, 20 °C), containing 100 mM NaCl, are shown in Figure 3a. The presence of ATP significantly shifts the titration curves toward a higher DnaC concentration range, clearly indicating that both nucleotides efficiently compete for the same binding site on the protein. The dependence of the relative fluorescence increase, as a function the number of bound DnaC molecules per ATP, is shown in Figure 3b. The average degree of DnaC binding on ATP has been determined using eq 5. The plot is clearly nonlinear. It rises at low values of the degree of binding and levels off as the degree of binding increases. Such behavior indicates that, although ATP competes efficiently with MANT-ADP for the binding site, its affinity is lower than the affinity of the analogue (*33*). At the maximum value of the monitored fluorescence signal ($\Delta F_{max} = 1.55$), one DnaC molecule associates with one ATP.

In the studied system, we have a single DnaC molecule competing for two different ligands, MANT-ADP and ATP. Knowing the maximum stoichiometries of the considered complexes, the partition function of the total system, *Z*, is described by

$$Z = 1 + K_{\mathrm{MANT-ADP}}P_{\mathrm{F}} + K_{\mathrm{ATP}}P_{\mathrm{F}} \qquad (7)$$

where $K_{\mathrm{MANT-ADP}}$ is the binding constant for MANT-ADP, K_{ATP} is the binding constant for ATP, and P_{F} is the free concentration of the DnaC protein. The concentration of the bound DnaC protein is then defined by

$$P_{\mathrm{b}} = \left(\frac{K_{\mathrm{MANT-ADP}}P_{\mathrm{F}}}{1 + K_{\mathrm{MANT-ADP}}P_{\mathrm{F}}}\right)[\mathrm{MANT-ADP}]_{\mathrm{Tot}} + \left(\frac{K_{\mathrm{ATP}}P_{\mathrm{F}}}{1 + K_{\mathrm{ATP}}P_{\mathrm{F}}}\right)[\mathrm{ATP}]_{\mathrm{Tot}} \qquad (8)$$

and

$$P_{\mathrm{b}} = (\sum\Theta_i)_{\mathrm{MANT-ADP}}[\mathrm{MANT-ADP}]_{\mathrm{Tot}} + (\sum\Theta_i)_{\mathrm{ATP}}[\mathrm{ATP}]_{\mathrm{Tot}} \qquad (9)$$

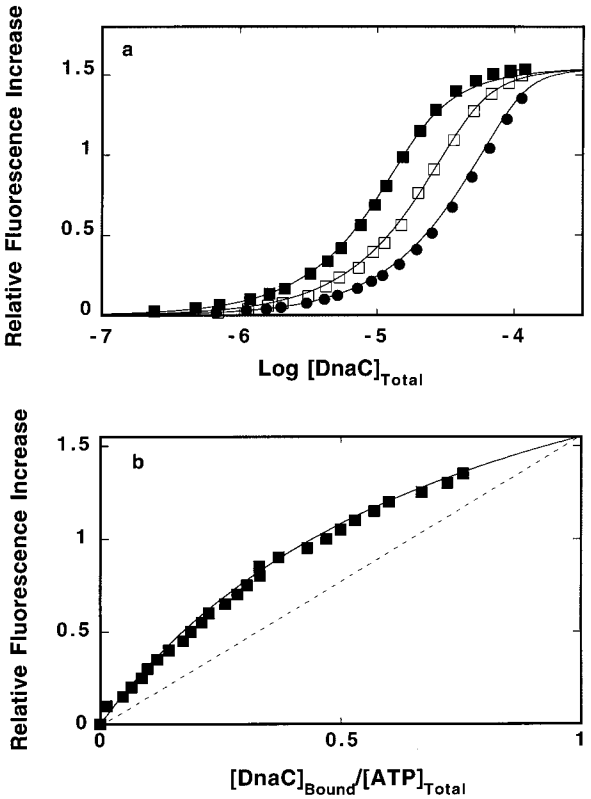

FIGURE 3: (a) Fluorescence titration of MANT-ADP with the DnaC protein, in buffer T4 (pH 8.1, 20 °C) containing 100 mM NaCl, at two different concentrations of the competing ligand, ATP: (□) 3.34×10^{-5} M; (●) 9.4×10^{-5} M. The titration in the absence of ATP is also included (■). The concentration of the reference ligand, MANT-ADP, is 1.5×10^{-5} M. The solid lines are computer fits of the titration curves with a single set of binding parameters, the ATP binding constant $K_{\mathrm{ATP}} = 1.3 \times 10^5$ M^{-1}, the MANT-ADP binding constant $K_{\mathrm{MANT-ADP}} = 3 \times 10^5$ M^{-1}, and $\Delta F_{max} = 1.55$. (b) Dependence of the relative fluorescence increase of MANT-ADP, ΔF, upon the average degree of binding of the DnaC protein on ATP, $[\mathrm{DnaC}]_{\mathrm{Bound}}/[\mathrm{ATP}]_{\mathrm{Tot}} = (\sum\Theta_i)_{\mathrm{ATP}}$ (■). The values of $(\sum\Theta_i)_{\mathrm{ATP}}$ have been determined using thermodynamically rigorous MCT approach described in Materials and Methods section. The solid line is the computer simulation of ΔF dependence upon $(\sum\Theta_i)_{\mathrm{ATP}}$ using eqs 7−9, with the determined values of $K_{\mathrm{ATP}} = 1.3 \times 10^5$ M^{-1}, $K_{\mathrm{MANT-ADP}} = 3 \times 10^5$ M^{-1}, and $\Delta F_{max} = 1.55$. The dashed line is the dependence of ΔF upon the average degree of binding of the DnaC protein on MANT-ADP.

where $[\mathrm{MANT-ADP}]_{\mathrm{Tot}}$ and $[\mathrm{ATP}]_{\mathrm{Tot}}$ are the total concentrations of MANT-ADP and ATP, respectively. The solid lines in Figure 3a are computer fits of the experimental isotherms using eqs 8 and 9, with $\Delta F_{max} = 1.55$, $K_{\mathrm{MANT-ADP}} = 3 \times 10^5$ M^{-1} and with a single fitting parameter K_{ATP}. The obtained value of $K_{\mathrm{ATP}} = (1.3 \pm 0.3) \times 10^5$ M^{-1}. The solid line in Figure 3b is the computer simulation of the observed fluorescence change of the reference nucleotide, MANT-ADP, as a function of the degree of binding of the DnaC protein on ATP, using the determined binding constants for MANT-ADP and ATP.

Analogous fluorescence titrations of MANT-ADP with the DnaC protein, in the presence of different concentrations of ADP, have been performed (data not shown). As in the case of ATP, the presence of ADP shifts the titration curves toward a higher DnaC concentration range as a result of the competition for the same binding site on the protein between the reference ligand, MANT-ADP, and ADP. The dependence of the relative fluorescence increase as a function of

Table 1: Thermodynamic and Spectroscopic Parameters for the Binding of MANT-ATP, MANT-ADP, ATP, and ADP to the *E. coli* DnaC Protein in Buffer T4 (pH 8.1, 20 °C) Containing 100 mM NaCl (see text for details)[a]

	MANT-ATP	MANT-ADP	ATP[b]	ADP[b]
K_N (M^{-1})	$(3 \pm 0.4) \times 10^5$	$(3 \pm 0.4) \times 10^5$	$(1.3 \pm 0.3) \times 10^5$	$(1.3 \pm 0.3) \times 10^5$
stoichiometry	1	1	1	1
ΔF_{max}	1.8 ± 0.1	1.5 ± 0.1		

[a] Errors are standard deviations determined using three and four independent titration experiments. [b] Determined using the MCT Method (*33*).

Table 2: Equilibrium Binding Constants, K_N, and Stoichiometries for the Binding of Different ATP and ADP Analogs to the *E. coli* DnaC Protein, Determined Using the MCT Method, in Buffer T4 (pH 8.1, 20 °C) Containing 100 mM NaCl (see text for details)

nucleotide	AMP−PNP	ATPγS	AMP−PCP	dATP	dADP
K_N (M^{-1})	$(4.5 \pm 1) \times 10^3$	$(1.2 \pm 0.5) \times 10^5$	ND[a]	$(3.8 \pm 0.5) \times 10^3$	$(1.8 \pm 0.5) \times 10^3$
stoichiometry	1	1	ND[a]	1	1

[a] ND, not determined. Affinity below the detection method in applied solution conditions ($K_N < 5 \times 10^2$ M^{-1}).

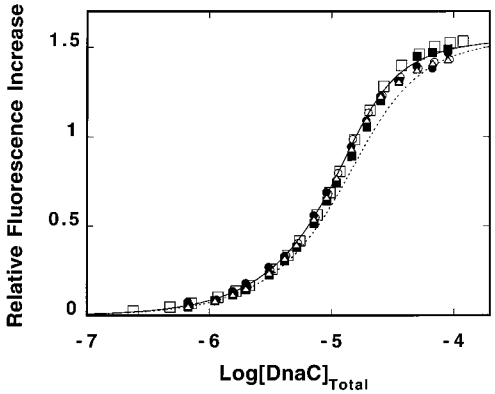

FIGURE 4: (a) Fluorescence titration of MANT-ADP with the DnaC protein, in buffer T4 (pH 8.1, 20 °C), containing 100 mM NaCl, in the absence (□) and presence of different competing nucleotide triphosphates: (●) GTP; (○) CTP; (△) TTP; (■) UTP. The concentration of the reference ligand, MANT-ADP, is 1.5×10^{-5} M. The concentrations of each of the competing nucleotides are 1×10^{-3} M. The dashed line is the theoretical titration curve at the same reference ligand (MANT-ADP) concentration (1.5×10^{-5} M) in the presence of a competing nucleotide (1 mM), having the intrinsic binding constant $K = 8 \times 10^2$ M^{-1}.

the number of bound DnaC molecules per ADP shows that one DnaC monomer binds to a single ADP molecule. The formation of the complex is characterized by $K_{ADP} = (1.3 \pm 0.3) \times 10^5$ M^{-1}. Thus, the obtained values of K_{ATP} and K_{ADP} directly show that both ATP and ADP have, within experimental accuracy, the same affinity for the nucleotide-binding site on the DnaC protein which is in excellent agreement with the results obtained using MANT-ATP and MANT-ADP (Table 1).

Base Specificity of the Nucleotide-Binding Site of the DnaC Protein. Ligand competition studies can provide a direct estimate of the base specificity of the nucleotide-binding site of the DnaC protein. Fluorescence titrations of MANT-ADP with the DnaC protein in the presence of different nucleotide triphosphates, GTP, CTP, TTP, and UTP in buffer T4 (pH 8.1, 20 °C), containing 100 mM NaCl, are shown in Figure 4. All titration curves, obtained in the presence of 1×10^{-3} M concentrations of each nucleotide, are, within experimental accuracy, completely superimposable on the MANT-ADP titration curve, indicating a very low, if any, affinity for the binding site. For comparison, a dashed line is included in Figure 4, which is a theoretical isotherm with the affinity of the ligand $K = 8 \times 10^2$ M^{-1}. It is evident that the affinities of all studied nucleotides must be about an order of magnitude lower than 8×10^2 M^{-1} to account for the lack of any competition effect at these high nucleotide phosphate concentrations (1×10^{-3} M). In other words, the binding constants for the nucleotide phosphates must be at least ~3−4 orders of magnitude lower than the intrinsic affinity of ATP. We have also performed direct fluorescence titrations of the MANT-GDP, MANT-CDP, and MANT-UDP with the DnaC protein in buffer T4 (pH 8.1, 20 °C), containing 100 mM NaCl (data not shown). The affinities of all studied MANT-analogues were undetectable in our solution conditions. Thus, these data clearly show that the nucleotide-binding site of the DnaC protein is very highly specific for the adenosine nucleotides (see Discussion).

Role of Phosphate Groups and Ribose in Interactions of Adenosine Nucleotides with the DnaC Protein. The fact that ATP and ADP have the same affinities for the nucleotide-binding site, but only ATP can induce a high-affinity state of the DnaC protein for the DnaB helicase (*3*, *9*, *13*, *14*), suggests that the γ-phosphate is involved in the complex allosteric interactions extending beyond the nucleotide-binding site (see Discussion). To address the question as to what extent the specific structure of the ATP phosphate group affects the energetics of the nucleotide binding, we performed competition titration studies using different ATP analogues: AMP−PNP, AMP−PCP, and ATP-γ-S. The analysis has been performed using MANT-ADP as a reference fluorescence ligand. The obtained thermodynamic parameters are included in Table 2.

The binding constant for AMP−PNP is $K_{AMP-PNP} = (4.5 \pm 1) \times 10^3$ M^{-1} which is ~2 orders of magnitude lower than $K_{ATP} = (1.3 \pm 0.3) \times 10^5$ M^{-1}. The affinity of the AMP−PCP is below the detection level of the method in our solution conditions. On the other hand, the affinity of ATP-γ-S is characterized by $K_{ATP-\gamma-S} = (1.2 \pm 0.5) \times 10^5$ M^{-1}, which, within experimental accuracy, is the same as K_{ATP}. Thus, replacement of a single oxygen atom in the phosphate group causes dramatic differences in the affinities of different adenosine triphosphate analogues (Table 2). Such differences of affinities are rather unexpected in light of the fact that the studied analogues have affinities comparable with ATP for several different ATPases, including the DnaB helicase (*33*, *39*−*41*). The large difference between the analogues and ATP, observed here for DnaC, must reflect a very different nature of the adenosine nucleotide-binding site of the DnaC protein (see Discussion).

To address the role of the sugar moiety in the binding of the adenosine nucleotides to the DnaC protein, we performed competition studies with dATP and dADP using MANT-ADP as a reference fluorescence cofactor. The obtained binding constants are included in Table 2. It is evident that the replacement of the ribose by deoxyribose has a profound effect on the nucleotide affinity. The binding constants for dATP and dADP are $K_{dATP} = (3.8 \pm 0.5) \times 10^3\ M^{-1}$ and $K_{dADP} = (1.8 \pm 0.5) \times 10^3\ M^{-1}$, respectively. These values are ~2 orders of magnitude lower than the binding constant of ATP and ADP. Thus, low values of K_{dATP} and K_{dADP} indicate that the ribose 2′ OH group actively participates in the interactions in the nucleotide-binding site. In this context, it is interesting that the MANT-group, which is located on the ribose, has very little effect on the energetics of the nucleotide binding (Figures 1 and 2). The small effect is not specific for the MANT derivatives. Another ATP analogue, TNP-ATP, which has the modifying group located on the ribose, also has an affinity of ~2 orders of magnitude higher than the affinity of dATP (data not shown). Both MANT- and TNP-analogues may undergo acyl migration, i.e., the analogues may exist in an equilibrium mixture of 2′ and 3′ isomers where the modifying group is located at the 2′ or 3′ oxygen of the ribose (*28*, *29*, *31*, *42*). Much higher affinities of both analogues, as compared to dATP, indicate that the fluorescent label must be predominantly located at the 3′ oxygen of the ribose (see Discussion).

Salt Effect on the ATP and ADP Analogues Binding to the DnaC Protein. The effect of salt on the energetics of the ATP and ADP binding to the DnaC protein has been examined using MANT-ATP and MANT-ADP analogues. Fluorescence titrations of MANT-ATP with the DnaC protein, in buffer T4 (pH 8.1, 20 °C), containing different NaCl concentrations, are shown in Figure 5a. Analogous titrations in the presence of NaBr are shown in Figure 5b. There is a decrease of the maximum fluorescence increase at saturation, ΔF_{max}, from 1.9 ± 0.1 at 50 mM to 1.7 ± 0.2 at 800 mM NaCl, indicating changes in the structure of the protein−nucleotide complex, as the salt concentration increases. The solid lines in Figure 5, panels a and b are computer fits to the single-site binding model with two fitting parameters, binding constant, $K_{MANT-ATP}$, and the maximum relative fluorescence increase, ΔF_{max} (eq 6). Figure 5c shows the dependence of the MANT-ATP intrinsic binding constant on NaCl and NaBr concentrations [log−log plots (*43*, *44*)]. The plots are linear and characterized by the slopes $\partial \log K/\partial \log[NaCl] = -0.7 \pm 0.1$ and $\partial \log K/\partial \log[NaBr] = -0.8 \pm 0.1$, respectively. The values of both slopes indicate that there is a net release of ~1 ion upon the complex formation and the release is independent of the type of anion in solution. However, although the slopes are very similar, there is an anion effect on the interactions reflected in the intrinsic binding constant, which is lower by a factor of ~1.5 in the presence of NaBr, when compared with the binding constant in the corresponding NaCl concentrations.

Examination of the salt effect on the binding of MANT-ADP to the DnaC protein has been performed in an analogous way (data not shown). The obtained log−log plots are linear in the studied salt concentration range and are characterized by the slopes $\partial \log K/\partial \log[NaCl] = -1 \pm 0.1$ and $\partial \log K/\partial \log[NaBr] = -0.9 \pm 0.1$, respectively. Thus, although the ADP analogue has one negatively charged phosphate group less than the ATP analogue, there is a net release of ~1 ion upon the complex formation between MANT-ADP and the DnaC protein. Moreover, similar to MANT-ATP, the number of ions released is independent of the type of anion in solution, although there is an anion effect on the interactions reflected in the slightly lower intrinsic binding constant in the presence of NaBr.

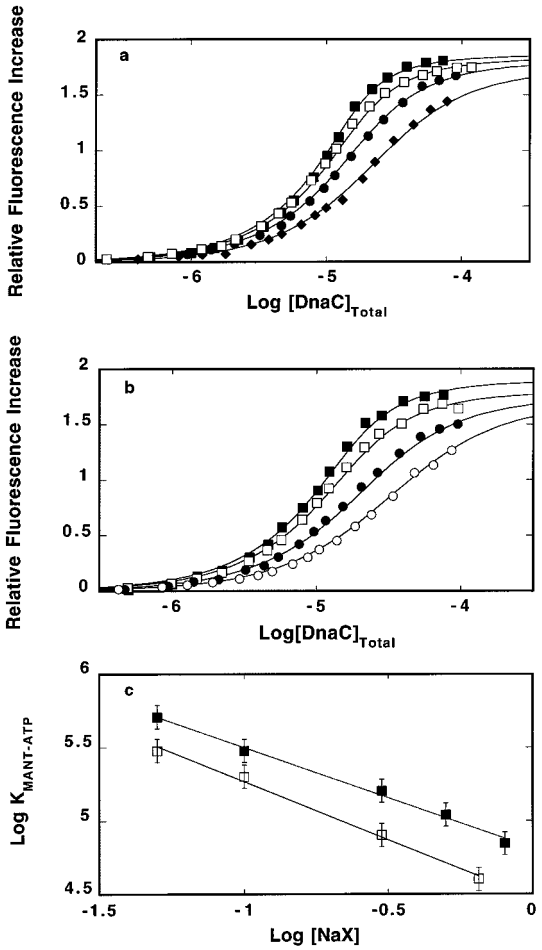

FIGURE 5: (a) Fluorescence titrations of MANT-ATP with the DnaC protein (λ_{ex} = 356 nm, λ_{em} = 450 nm) in buffer T4 (pH 8.1, 20 °C), containing different NaCl concentrations: 50 mM (■); 100 mM (□); 300 mM (●); 800 mM (◆). The solid lines are computer fits of the titration curves, using the single-site binding isotherm (eq 6) with two fitting parameters, $K_{MANT-ATP}$ and ΔF_{max}. (b) Fluorescence titrations of MANT-ATP with the DnaC protein (λ_{ex} = 356 nm, λ_{em} = 450 nm) in buffer T4 (pH 8.1, 20 °C) containing different NaBr concentrations: 50 mM (■); 100 mM (□); 300 mM (●); 650 mM (○). The solid lines are computer fits of the titration curves, using the single-site binding isotherm (eq 6) with two fitting parameters, $K_{MANT-ATP}$ and ΔF_{max}. (c) The dependence of the logarithm of the binding constant, $K_{MANT-ATP}$, upon the logarithm of NaCl (■) or NaBr (□) concentrations. The solid lines are linear least-squares fits which provide the slopes $\partial \log K_{MANT-ATP}/\partial \log[NaCl] = -0.7 \pm 0.1$ and $\partial \log K_{MANT-ATP}/\partial \log[NaBr] = -0.8 \pm 0.1$, respectively.

Magnesium Effect on the Binding of ATP and ADP Analogues to the DnaC Protein. Experiments described in the previous sections were performed in buffer T4 that contains 5 mM $MgCl_2$. The data showed that, in the presence of magnesium, the energetics of the ATP and ADP analogues are similarly affected by a monovalent salt in the solution. Fluorescence titrations of MANT-ATP and MANT-ADP with the DnaC protein in buffer T4 (pH 8.1, 20 °C), containing 100 mM NaCl, but in the absence of $MgCl_2$, are

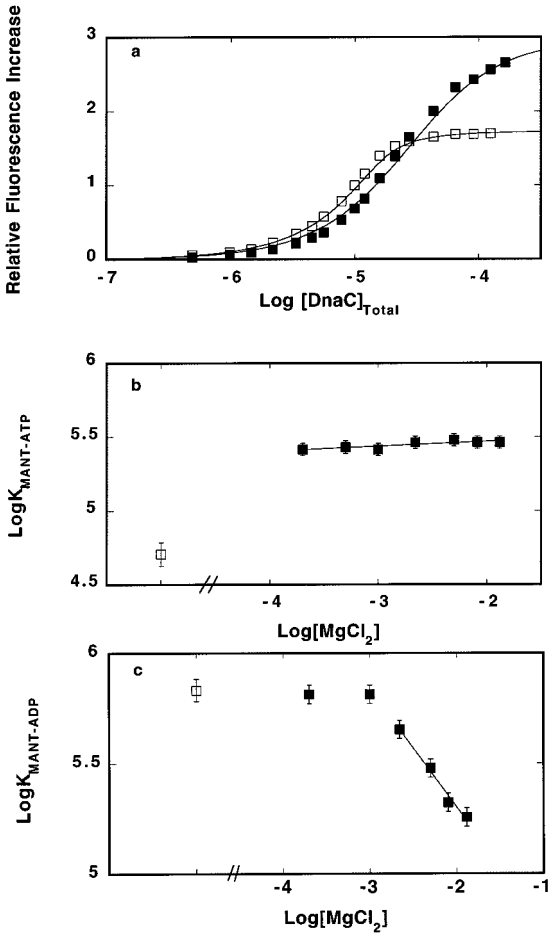

FIGURE 6: (a) Fluorescence titrations of MANT-ATP (■) and MANT-ADP (□) with the DnaC protein (λ_{ex} = 356 nm, λ_{em} = 450 nm) in buffer T4 (pH 8.1, 20 °C), in the absence of $MgCl_2$. The concentrations of both nucleotide analogues are 1.5×10^{-5} M. The solid lines are the computer fits of the experimental isotherms to a single-site binding isotherm (eq 6) using two fitting parameters, binding constant K_N and the maximum relative fluorescence increase, ΔF_{max}, which provide: $K_{MANT-ATP} = 5.1 \times 10^4$ M^{-1}, $\Delta F_{max} = 3$, and $K_{MANT-ADP} = 6.8 \times 10^5$ M^{-1}, and $\Delta F_{max} = 1.73$, respectively. (b) The dependence of the logarithm of the binding constant, $K_{MANT-ATP}$, upon the logarithm of the $MgCl_2$ concentration (■). The solid line is the linear least-squares fit of the plot which provides the slope $\partial \log K_{MANT-ADP}/\partial \log[MgCl_2] = 0.03 \pm 0.1$. (c) The dependence of the logarithm of the intrinsic binding constant, $K_{MANT-ADP}$, upon the logarithm of the $MgCl_2$ concentration (■). The solid line is the linear least-squares fit of the liner part of the plot at high $MgCl_2$ concentration range, which provides the slope $\partial \log K_{MANT-ADP}/\partial \log[MgCl_2] = -0.5 \pm 0.1$. The open square (□) corresponds to the value of binding constants determined in the absence of $MgCl_2$.

shown in Figure 6a. It is clear that both MANT-ATP and MANT-ADP bind the DnaC protein in the absence of magnesium. However, there are now significant differences between the cofactors. The maximum relative fluorescence increase of MANT-ADP upon saturation with the DnaC protein is $\Delta F_{max} = 1.7 \pm 0.15$, which is only ~10% higher than ΔF_{max}, obtained in the presence of 5 mM $MgCl_2$ (Figure 2). On the other hand, the value of ΔF_{max} for MANT-ATP is 3 ± 0.3, which is ~70% higher than the value obtained in the presence magnesium (Figure 1a). The large difference in the observed fluorescence increase indicates that Mg^{2+} cations strongly affect the structure of the ATP complex with the DnaC protein but not the complex with ADP (see Discussion). The solid lines in Figure 6a are computer fits to a single-site binding isotherm (eq 6) with two fitting parameters, binding constant, K, and the maximum relative fluorescence increase, ΔF_{max}. The obtained values of the binding constant and ΔF_{max} are $K_{MANT-ATP} = (5.1 \pm 0.6) \times 10^4$ M^{-1}, and $K_{MANT-ADP} = (6.8 \pm 0.8) \times 10^5$ M^{-1} for MANT-ATP and MANT-ADP, respectively. Thus, in the absence of $MgCl_2$, not only is the structure different, but also the affinity of the ATP analogue is lower by a factor of ~6 than in the presence of magnesium. On the other hand, the binding constant of MANT-ADP is increased by a factor of ~2, as compared to the value determined in the presence of 5 mM $MgCl_2$.

The dependence of the binding constant of MANT-ATP upon the logarithm of the $MgCl_2$ concentration is shown in Figure 6b. Even at the lowest [$MgCl_2$] examined, 2×10^{-4} M, the binding constant reaches the same value as the values obtained at high $MgCl_2$ concentrations. Such behavior indicates that the binding site (sites) of magnesium cations, affecting the structure and affinity of the ATP analogue, must have an affinity of $> 3 \times 10^4$ M^{-1}. Thus, the binding of MANT-ATP is affected by a specific, high affinity magnesium binding. In the high [$MgCl_2$] range, the plot, within experimental accuracy, is linear and characterized by the slope ~0 ($\partial \log K_{MANT-ATP}/\partial \log[MgCl_2] = 0.03 \pm 0.1$). This suggests that even at this [$MgCl_2$] range there is an ion uptake in the binding process (see Discussion).

The dependence of the binding constant of MANT-ADP upon the logarithm of the $MgCl_2$ concentration, shown in Figure 6c is very different. The plot is clearly nonlinear. At low a [$MgCl_2$] range, the binding constant is not affected by the increasing [$MgCl_2$] and the slope $\partial \log K_{MANT-ADP}/\partial \log[MgCl_2] \approx 0$. Above ~1 mM [$MgCl_2$], the value of the binding constant strongly decreases and the plot becomes linear and characterized by the slope $\partial \log K_{MANT-ADP}/\partial \log[MgCl_2] = -0.5 \pm 0.1$. Thus, the binding process of MANT-ADP is accompanied by the net ion release (see Discussion).

DISCUSSION

Binding of nucleotide cofactors to the DnaC protein plays a crucial role in regulating the physiological activities of the protein, i.e., its interactions with the DnaB helicase and subsequent recognition of the replication fork and primosome machinery (*1*−*5*). Yet, little is known about the molecular mechanism of the DnaC−nucleotide interactions. In this communication, we describe, for the first time, quantitative studies of the stoichiometry, free energy of binding, specificity, and effects of solution conditions on DnaC protein interactions with nucleotide cofactors. In our studies, we used the DnaC protein with a sequence exactly corresponding to the wild-type sequence of the protein (*23*). Moreover, the measurement of the protein extinction coefficient allowed us to determine the exact concentration of the protein necessary for the quantitative analysis of the binding processes.

DnaC Protein Has a Single Nucleotide-Binding Site. The thermodynamic studies have greatly been facilitated by the finding that the association of the MANT-analogues of the nucleotides with the DnaC protein is accompanied by a strong analogue fluorescence increase. Such a strong fluorescence change provides the necessary signal for high-resolution thermodynamic studies to obtain the correct

stoichiometries and affinities of the formed complexes. A similar effect on the fluorescence of nucleotide analogues has been previously found in the case of the *E. coli* DnaB helicase and was extensively used by us to quantitatively examine the structure, thermodynamics, and kinetics of the DnaB helicase interactions with the cofactors (*30*, *32*, *33*, *37*, *45*).

Previous estimates of the stoichiometry of the DnaC protein−nucleotide complex, obtained using the gel filtration technique, provided a value of ∼0.6 ATP molecule bound/DnaC monomer (*9*). The authors assumed the presence of 50% of the inactive protein and concluded that the stoichiometry of the complex is 1.3 nucleotides/DnaC. Using the thermodynamically rigorous fluorescence titration method (see above), we established that at saturation the DnaC protein binds a single molecule of MANT-ATP and MANT-ADP. Moreover, analogous thermodynamic analysis of the binding of unmodified ATP and ADP to DnaC shows a 1:1 stoichiometry of the complexes (Figure 3; Table 1). Thus, the DnaC protein has a single nucleotide-binding site.

ATP and ADP Have the Same Affinities for the Nucleotide-Binding Site of the DnaC Protein. Experiments with MANT-ATP, MANT-ADP, and unmodified ATP and ADP show that in the presence of magnesium both ATP and ADP have the same affinities for the DnaC nucleotide-binding site. This is an interesting and surprising aspect of DnaC protein interactions with nucleotide cofactors. Recall, binding of ATP to the DnaC protein is specifically required for the formation of a stable DnaB helicase−DnaC protein complex (*9*). ADP does not support this reaction. Our results show that the difference between ATP and ADP in affecting the DnaC−DnaB interactions simply does not result from the low affinity of ADP for the binding site. Rather, the data indicate that the presence of the γ-phosphate is necessary to induce a specific allosteric transition of the DnaC protein leading to a dramatic increase of its affinity for the DnaB helicase. Energetically, such a mechanism would rely on the use of part of the free energy of ATP binding to induce the conformational transition of the DnaC protein, thus lowering the observed affinity of the adenosine triphosphate. The free energy of ADP binding does not contain the extra expenditure used to induce conformational transition of the protein and, as a result, its affinity is unaffected. In this context, different fluorescence changes accompanying the binding of MANT-ATP and MANT-ADP most probably reflect the different conformational states of the protein−cofactor complexes. Quantitative structural and kinetic studies of the nucleotide binding to the DnaC protein are necessary to obtain further insight into the internal energetics of the binding process (*46*−*48*).

Nucleotide-Binding Site of the DnaC Protein Is Highly Specific for Adenosine Cofactors. Quantitative competition studies of the binding of different nucleotide triphosphates, GTP, CTP, TTP, UTP, MANT-GDP, MANT-CDP, and MANT-UDP show that the affinities of these cofactors are, if any, ∼3−4 orders of magnitude lower than the affinities of the corresponding adenosine nucleotides. These data unambiguously show that the nucleotide-binding site of the DnaC protein is highly specific for the adenosine nucleotides (Figures 4). The base specificity of the DnaC nucleotide-binding site has previously been the subject of a significant controversy (*9*, *27*). Wahle et al. did not see any competition between GTP and ATP for the binding site, using the equilibrium gel filtration technique (*9*). Moreover, only ATP supported the formation of the DnaC−DnaB complex formation. On the other hand, lack of any base specificity has been reported on the bases of photo-cross-linking efficiency (*27*). Our quantitative results are in excellent agreement with the qualitative conclusions of Wahle et al. and refute the photo-cross-linking findings (*27*). It should be pointed out that covalent photo-cross-linking is a nonspecific, nonequilibrium technique which may cause artifacts if proper precautions are not taken into account, particularly the time of UV radiation exposure and a very pure protein preparation. The purity and method of determination of the DnaC protein concentration were not included in the experimental protocols reported by these authors (*27*).

The physiological role of the DnaC protein is strictly related to its ability to form a very specific complex with the *E. coli* primary replicative helicase, the DnaB protein (*1*, *2*, *11*−*14*). Yet, the results obtained in this work show that the ATP/ADP-binding site on the DnaC protein is very different from the nucleotide-binding site of the DnaB helicase (*49*). The DnaB helicase is a potent ATPase, even in the absence of the ssDNA (*30*). The nucleotide-binding site of the protein can accept all four ribonucleotides with some preference for purine cofactors (*30*, *33*). The affinity for deoxyribonucleotides, dATP and dADP, is similar to that of the ribose cofactors (*33*). Both AMP−PCP and AMP−PNP have substantial affinities for the helicase nucleotide-binding sites. All these data indicate that the presence of 2′ oxygen and the structure of the triphosphate group are important for catalysis by the helicase, but not for ground-state interactions with the enzyme.

On the other hand, the nucleotide-binding site on the DnaC protein shows high specificity for the adenosine nucleotides and a lack of intrinsic ATPase activity. Moreover, the deoxyribonucleotides and ATP analogues, AMP−PCP and AMP−PNP, have dramatically lower affinities for the DnaC nucleotide binding site, as compared to ATP and ADP, indicating that both the 2′ oxygen and the structure of the phosphate group play important roles in ground-state interactions in the binding site. Current data indicate that the DnaC protein forms a complex with the DnaB helicase in which six DnaC monomers associate with a single DnaB hexamer, a process which is controlled by the ATP binding to the DnaC protein (*9*, *10*). Thus, the complex $(DnaC)_6$:$(DnaB)_6$ contains two sets of six nucleotide binding sites with very different properties. The exact role of both sets of very different nucleotide-binding sites in the functioning of the $(DnaC)_6$:$(DnaB)_6$ complex is still unknown.

On the basis of chemical studies, MANT-ATP and TNP-ATP, whose modification is located on the ribose, was originally postulated to exist solely as 3′ isomers (*28*, *29*). However, both analogues can exist as 2′ or 3′ forms, due to the acyl migration between the two oxygen atoms of the ribose. NMR studies indicate that MANT-derivatives exist as a mixture of 2′ and 3′ isomers, with the 3′ isomer being significantly predominant (*42*). Our fluorescence quantum yield measurements of the MANT-ADP and MANT-dADP also indicate that the 3′ isomer is a dominant form (*31*). In this context, the affinities of MANT- and TNP- analogues, similar to the affinity of the unmodified nucleotides, result from the fact that both analogues exist in solution predomi-

nantly as 3′ isomers, leaving the 2′ oxygen free to engage in interactions with the binding site.

The major similarity between the DnaB and DnaC nucleotide-binding sites is their hydrophobic nature. Emission of the MANT-group is very sensitive to the polarity of the environment, strongly increasing with the decreasing polarity (*28*−*31*). We have previously used this property of the analogues to quantitatively assess the polarity of the nucleotide-binding site of the DnaB helicase (*31*). The fluorescence emissions of both MANT-derivatives is strongly increased upon binding to the DnaC (Figures 1 and 2). A similar, strong increase of TNP-ATP fluorescence occurs upon saturation with the DnaC protein (data not shown). Although the fluorescence increases of MANT-analogues are not as pronounced as in the case of the DnaB helicase, nevertheless, they clearly indicate that the environment of the binding site is predominantly hydrophobic (*30*, *31*).

Both MANT-ATP and MANT-ADP show, within experimental accuracy, the same dependence of their affinities upon the monovalent salt in solution, independently of anion type, although the anion effect is evident in the lower binding constants in the presence of NaBr as compared to NaCl (Figure 5). This is rather surprising because Br^- has a significantly higher affinity for the protein amine groups than Cl^-, thus, indicating that anion-binding sites are already saturated with Cl^- and Br^- at the lowest salt concentrations used in our experiments (*50*). Recall, the maximum fluorescence increase, ΔF_{max}, of the DnaC−MANT-ATP complex has a higher value than the ΔF_{max} observed for MANT-ADP, indicating different structures of both complexes (Figures 1 and 2). Moreover, only the DnaC−ATP complex has a high affinity for the DnaB helicase (*9*, *10*). These results strongly suggest that the structural differences between the DnaC−ATP and DnaC−ADP complexes, evident in the much higher affinity of the ATP−DnaC complex for the DnaB helicase and the higher fluorescence changes accompanying the binding, are not thermodynamically linked to the release of monovalent ions from the complexes.

Contrary to monovalent salts, magnesium cations exert a distinct effect on the binding of ATP and ADP analogues to the DnaC protein. Although neither ATP nor ADP requires Mg^{2+} to bind the nucleotide-binding site of the DnaC protein, the interactions of the MANT-ATP with the binding site are strongly affected by Mg^{2+} cations (Figure 6a). In the absence of Mg^{2+}, the affinity is significantly lower and the observed ΔF_{max} is dramatically higher than in the presence of magnesium cations. The decrease of ΔF_{max} in the presence of $MgCl_2$ indicates that, as a result of the conformational transition, the ribose region of the nucleotide is shifted into a much less hydrophobic environment when the protein is saturated with Mg^{2+} (*30*, *31*). The magnesium effect is completely saturated at the lowest [$MgCl_2$] examined (2×10^{-4} M), indicating that the binding of the ATP analogue is affected by the high affinity magnesium binding sites, with a binding constant larger than 3×10^4 M^{-1}. It is interesting that a further increase of [$MgCl_2$] does not decrease the affinity of MANT-ATP for the nucleotide-binding site. A zero or a slightly positive value of the slope of the log−log plot at elevated [$MgCl_2$] suggests that an additional Mg^{2+} cation uptake, to lower affinity cation-binding sites, occurs in the ATP analogue binding process (Figure 6b).

The effect of magnesium on MANT-ADP binding to the DnaC protein is diametrically opposite from MANT-ATP. In the absence of magnesium, the affinity is higher by a factor of ∼2. The relative fluorescence increase is only slightly higher in the presence of $MgCl_2$, indicating that, contrary to MANT-ATP, the conformation of the ADP analogue−binding site complex is not significantly affected by the Mg^{2+} cation binding to strong magnesium binding sites (Figure 6c). The linear part of the log−log plot, at a high $MgCl_2$ concentration range, is characterized by the slope, $\partial \log K / \partial \log[MgCl_2] = -0.5 \pm 0.1$, which indicates that a net ion release accompanies the binding of the ADP analogue. In other words, the data indicate that ADP and magnesium cations compete for the binding site. Above ∼1 mM [$MgCl_2$], the binding constant of the ADP analogue decreases with the increase of [$MgCl_2$] which strongly suggests that the ion release occurs from cation-binding sites characterized by the affinity constant of $\sim 10^3$ M^{-1}. However, these low-affinity sites do not affect ATP analogue binding (Figure 6b).

A dramatic opposite effect of magnesium on the complexes of the DnaC protein with MANT-ATP and MANT-ADP provides strong evidence that the structure of the complexes and interactions of the ATP and ADP analogues, with the nucleotide-binding site of the DnaC protein, are substantially different. This is despite very similar affinities of both nucleotides. The obtained data indicate that the complexes of the DnaC protein with nucleotide cofactors are specifically controlled by magnesium cation binding to the protein, i.e., through allosteric interactions between the magnesium and the nucleotide binding sites.

Although nucleotides are often treated as "small" ligands, they are complex molecules with distinctive structural regions (base, sugar, phosphates). Each of these regions can be responsible for triggering specific responses in the protein and control its activities, either independently or in a concerted way. The results described in this work indicate that the nucleotide affinity for the DnaC-binding site includes the recognition of all three major structural elements of the cofactor, the base, ribose, β-, and γ-phosphate groups. Moreover, magnesium cations play an important part in these recognition processes. The presence of only two of these structural elements results in a dramatic decrease of affinity and an inability to form a complex with the binding site of the protein. However, efficient association with the binding site of DnaC is not enough to trigger specific conformational changes of the entire protein leading to an increased affinity toward the DnaB helicase. Thus, both ATP and ADP have the same affinities for the nucleotide-binding site of the DnaC protein, yet, only ATP can induce high affinity toward the helicase. Our results strongly suggest that the nucleotide-binding site, as well as the entire protein, are complex, coupled allosteric systems in which conformational changes are triggered by subtle, specific interplay between the nucleotide and magnesium binding sites, and are extended to the rest of the protein. The quantitative mechanism of these interactions is currently being studied in our laboratory.

ACKNOWLEDGMENT

We wish to thank Dr. Maria J. Jezewska for very helpful discussions concerning this project and Gloria Drennan Davis for her help in preparing the manuscript.

REFERENCES

1. Kornberg, A., and Baker, T. A. (1992) *DNA Replication*, Freeman, San Francisco.
2. Marians, K. J. (1992) *Annu. Rev. Biochem. 61*, 673−719.
3. Skarstad, K., and Wold, S. (1995) *Mol. Microbiol. 17*, 825−831.
4. Wickner, S., Wright, M., and Hurwitz, J. (1973) *Proc. Natl. Acad. Sci. U.S.A. 71*, 783−787.
5. Wickner, S., and Hurwitz, J. (1974) *Proc. Natl. Acad. Sci. U.S.A. 72*, 921−925.
6. Wechsler, J. (1975) *J. Bacteriol. 121*, 594−599.
7. Wechsler, J., and Gross, J. D. (1971) *Mol. Gen. Genet. 113*, 273−284.
8. Marians, K. J. (1999) *Prog. Nucleic Acids Res. Mol. Biol. 63*, 39−67.
9. Wahle, E., Lasken, R. S., and Kornberg, A. (1989) *J. Biol. Chem. 264*, 2463−2468.
10. Wahle, E., Lasken, R. S., and Kornberg, A. (1989) *J. Biol. Chem. 264*, 2469−2475.
11. Allen, G. C., and Kornberg, A. (1991) *J. Biol. Chem. 266*, 22096−22101.
12. Allen, G. C., and Kornberg, A. (1991) *J. Biol. Chem. 268*, 19204−19209.
13. Kobori, J. A., and Kornberg, A. (1982) *J. Biol. Chem. 257*, 13757−13762.
14. Kobori, J. A., and Kornberg, A. (1982) *J. Biol. Chem. 257*, 13763−13769.
15. Masai, H., and Arai, K. (1995) *Eur. J. Biochem. 230*, 384−395.
16. Bujalowski, W., and Jezewska, M. J. (1995) *Biochemistry 34*, 8513−8519.
17. Jezewska, M. J., and Bujalowski, W. (1996) *Biochemistry 35*, 2117−2128.
18. Jezewska, M. J., Kim, U.-S., and Bujalowski, W. (1996) *Biochemistry 36*, 2129−2145.
19. Jezewska, M. J., Rajendran S., Bujalowska, D., and Bujalowski, W. (1998) *J. Biol. Chem. 273*, 10515−10529.
20. Jezewska, M. J., Rajendran S., and Bujalowski. W. (1998) *J. Biol. Chem. 273*, 9058−9069.
21. Jezewska, M. J., Rajendran, S., and Bujalowski, W. (1997) *Biochemistry 36*, 10320−10326.
22. Sancar, A., and Hearst, J. E. (1993) *Science 259*, 1415−1420.
23. Nakayama, N., Arai, N., Bond, M. W., Miyajima, A., Kobori, J., and Arai, K. (1987) *J. Biol. Chem. 262*, 10475−10480.
24. Kobori, J. A., and Kornberg, A. (1982) *J. Biol. Chem. 257*, 13770−13775.
25. Lanka E., Geschke, B., and Schuster, H. (1978) *Proc. Natl. Acad. Sci. U.S.A. 75*, 799−803.
26. Lanka, E., and Schuster, H. (1983) *Nucleic Acid Res. 11*, 987−997.
27. Biswas, S. B., and Biswas, E. E. (1987) *J. Biol. Chem. 262*, 7831−7838.
28. Hiratsuka, T., and Uchida, K. (1973) *Biochim. Biophys. Acta 320*, 635−647.
29. Hiratsuka, T. (1983) *Biochim. Biophys. Acta 742*, 496−508.
30. Bujalowski, W., and Klonowska, M. M. (1993) *Biochemistry 32*, 5888−5900.
31. Bujalowski, W., and Klonowska, M. M. (1994) *Biochemistry 33*, 4682−4694.
32. Bujalowski, W., and Klonowska, M. M. (1994) *J. Biol. Chem. 269*, 31359−31371.
33. Jezewska, M., J., Kim, U.-S., and Bujalowski, W. *Biophys. J.* (1997) *71*, 2075−2086.
34. Edeldoch, H. (1967) *Biochemistry 6*, 1948−1954.
35. Gill, S. C., and von Hippel, P. H. (1989) *Anal. Biochem. 182*, 319−326.
36. Lakowicz, J. R. (1999) *Principle of Fluorescence Spectroscopy*, Plenum Press.
37. Jezewska, M. J., and Bujalowski, W. (1997) *Biophys. Chem. 64*, 253−269.
38. Jezewska, M. J., Rajendran, S., and Bujalowski, W. (1998) *Biochemistry 37*, 3116−3136.
39. Moore, J. K., and Lohman, T. M. (1994) *Biochemistry 33*, 14550−14564.
40. Shriver, J. W., and Sykes, B. D. (1981) *Biochemistry 20*, 2004−2012.
41. Granot, J., Mildvan, A. S., Bramson, H. N., and Kaiser, E. T. (1980) *Biochemistry 19*, 3537−3543.
42. Cremo, C. R., Neuron, J. M., and Yount, R. G. (1990) *Biochemistry 29*, 3309−3319.
43. Record, M. T., Jr., Anderson, C. F., and Lohman, T. M. (1978) *Q. Rev. Biophys. 11*, 103−178.
44. Record, M. T., Lohman, T. M., and deHaseth, P. L. (1976) *J. Mol. Biol. 107*, 145−158.
45. Bujalowski, W., Klonowska, M. M., and Jezewska, M. J. (1994) *J. Biol. Chem. 269*, 31350−31358.
46. Bujalowski, W., and Jezewska, M. J. (2000) *J. Mol. Biol. 295*, 831−852.
47. Bujalowski, W., and Jezewska, M. J. (2000) *Biochemistry 39*, 2106−2122.
48. Moore, J. K., and Lohman, T. M. (1994) *Biochemistry 33*, 14565−14578.
49. Koonin, E. V. (1992) *Nucleic Acids Res. 20*, 1997−1997.
50. Von Hippel, P. H., and Schleich T. (1969) in *Structure of Biological Macromolecules* (Timasheff, S., and Fasman, G. D., Eds.) Chapter 6, Marcel Dekker, New York.

BI0012484